J. Am. Ceram. Soc., 95 [10] 3016–3018 (2012)
DOI: 10.1111/j.1551-2916.2012.05395.x

journal
Rapid Communication

# High Strength Alumina Micro-Beams Fabricated by Inkjet Printing

Noah R. Philips,[§,*,†] Brett G. Compton,[‡,*] and Matthew R. Begley[§]

[‡]Materials Department, University of California, Santa Barbara, California

[§]Mechanical Engineering Department, University of California, Santa Barbara, California

**Freestanding ceramic microbeams were fabricated by inkjet printing of aqueous colloidal suspensions (up to 23 vol% alumina). Their high strength (920 MPa in bending) and stiffness ($E \approx 400$ GPa) is attributed to low porosity (void fraction 0.03) and a paucity of microstructural flaws. A range of ink compositions and beam thicknesses were printed using a commercial inkjet cartridge and isostatically compacted prior to firing.**

## I. Introduction

DIRECT printing of three-dimensional structures creates opportunities not only for rapid fabrication[1] but also for "materials by design," wherein material and component architectures are integrated to enhance performance.[2] Although various approaches have particular pros and cons,[3] direct multi-component ink-jet printing of materials has the capacity to create multiphase microstructures with discontinuous (yet spatially ordered) features and functional gradients. The native high resolution of inkjet lends itself to precise control of microstructure (critical for high performance composites) whereas the small nozzles perforce mitigate agglomerates (a typical strength limiting feature). This potential enables improved composite performance and microstructures that can be spatially integrated with component design.

Despite a decade of effort to develop direct-write inkjet manufacturing techniques for ceramics,[4] and substantial efforts to utilize structural materials,[3,5,6] there are very few reports on the connection between processing parameters, microstructure and mechanical properties.[7] The existing material printing literature largely addresses the formation of defects with special relevance to the reprographic heritage of the underlying technique. This article will focus on the mechanical properties of the fired ceramics and the dependence on microstructure defects that have a patent impact on material properties (e.g., crack-like voids, agglomerates, residual porosity), rather than the morphological issues (e.g., coffee rings,[8,9] line bulging,[10] feature size/drop spreading[11]).

Here, we demonstrate that high-strength submillimeter alumina structures can be made by limited modification of a low-cost inkjet printer, while maintaining the capacity for both large-scale printing and integration into composites.

## II. Experimental Procedure

Ceramic inks comprised aqueous colloidal suspensions (after Özkol *et al.*[12]) of high purity aluminum oxide powders with particle size 100–200 nm (AKP-50 alumina; Sumitomo, Tokyo, Japan), a polyacrylic acid dispersant (Duramax D-3005; Rohm & Haas, Philadelphia, PA), and ethylene glycol as a rheology modifier. The alumina powder was added to a continuously stirred aqueous mixture of $0.8\,mg/(m^2 Al_2O_3)$ dispersant and ethylene glycol (9 wt% after solids addition) to form three distinct ink compositions: 12.6, 17.4, and 23.2 vol % alumina (this corresponds to 36, 45, and 54 wt%).

Ink slurries were then mixed on a low energy ball mill with zirconia media for $\geq 24$ h. To eliminate agglomerates, a sedimentation protocol was employed as follows: inks were held in glass columns for 24 h to allow larger particles ($\gtrapprox 5\mu m$) to settle and low density organic impurities (e.g., lint) to float. The upper and lower deciles of the sedimented column were discarded and the remainder filtered through 5 μm membrane filters into pre-cleaned inkjet cartridges. Commercially available black ink cartridges (HP 45 ink, 51645A cartridges; Hewlett-Packard, Palo Alto, CA) were cleaned with detergent, rinsed with deionized water and (after refilling with ceramic ink) de-aired. The ink-loaded cartridges were then ready to print.

An HP 9300 inkjet printer was modified for 3D printing in two ways: by-passing of the paper feed function and installation of a heated stage. Due to limitations of the printer, accurate registration between printed layers required disabling the paper handling features, resulting in a single axis print system. As the printer required feedback from the undesired motion control systems,[13] a second printer was configured to execute the motion commands and return the appropriate feedback; this allowed the printer to function without further modification. A heated stage was installed in place of the customary print media. Printing was carried out with the stage at 60°C under flowing air.

Microbeams were printed from an image file with multiple copies of a single pixel line pattern such that layers of ink from a single nozzle could be built up with an arbitrary number of passes. Also included was a discrete (non-over printing) point for each successful print pass, creating a record of success or failure on each print pass for each nozzle (Fig. 1). Print substrates comprised alumina plates (ADS-96R; Coorstek, Golden, CO) coated with a graphite aerosol (Aerodag G; supplied by Ted Pella, Redding, CA) to form a release layer. To achieve a uniform and pinhole free coating, the substrate was dried between applications for a total of ≈5 coats. Following printing, microbeam specimens were cold isostatically pressed (while still on the alumina substrates) at 324 MPa and fired at 1400°C for 2 h under zirconia setter tiles in vacuum ($<10^{-3}$ Pa). Fired microbeams were then interlaminated between zirconia setter tiles to limit warpage, and fired 2 additional hours at 1400°C in air. Freestanding microbeams of macroscopic (>50 mm) length were recovered after the final firing operation. The beams were sufficiently robust as to be manipulated with tweezers or a gloved hand.

Residual porosity and grain size in the printed beams were determined using scanning electron microscopy (SEM) of

R. Ballarini—contributing editor

Manuscript No. 31568. Received June 15, 2012; approved November 07, 2012.
*Member, The American Ceramic Society.
†Author to whom correspondence should be addressed. e-mail: nphilips@engineering.ucsb.edu


**Fig. 1.** As-printed ceramic microbeams. At left, beams printed by the subsequent application of 50 layers of 17 vol% alumina ink. At right, each stripe provides a record of printing success for *all* nozzles at each print pass.

polished cross sections, whereas shape and surface roughness were assessed using interferometric profilometry (Wyko NT1110 Optical Profiling System; Veeco Instruments Inc., Plainview, NY). Mechanical properties were determined using cantilevers formed by gluing beams on a substrate (with the flat side mating). The specific modulus was determined using a piezoelectric actuator to excite the substrate with a step displacement input, with the beam's vibration response recorded with a non-contact laser displacement sensor. The temporal response of the cantilever end was deconvoluted to determine its natural frequency, which was then used to calculate specific modulus via standard formulae. The strength of the beams was calculated by measuring the flexural limit loads of the cantilever and the distance from the load point to the failure surface. Loading was applied to the narrow, curved side of the beam, near the free end (Fig. 4, inset). Cross-sectional area, moment of inertia, and centroid location were directly calculated (by numerical integration) from SEM images of fracture surfaces and virtual cross sections from profilometery data; the distance from the tensile surface to the centroid was determined by inspection. Primary fracture surfaces for observation were ensured by embedding beams in a water soluble grease (Phynal Grease, supplied by Wilmad LabGlass, Vineland, NJ) to suppress vibrations leading to secondary fractures.[14]

## III. Observations and Analysis

Interferometric measurements of surface profiles, shown in Fig. 2, revealed uniform shape and low surface roughness (arithmetic average of 3D roughness, $S_a < 1$ μm). The smooth surfaces, both top and bottom, illustrate the paucity of any large (>5 μm) defects from the printing operation. Progressive densification throughout the process can be seen in the virtual cross sections extracted from the topography (Fig. 2 inset). Inspection of polished cross sections [Fig. 3(a)] reveals low residual porosity (void volume fraction, $\phi = 0.03$) comprising small residual pores (90th percentile pore diameter, D90 ≈ 0.25 μm) that are uniformly dispersed and generally isotropic. The alumina grains are submicrometer and equiaxed ($d = 0.5$ μm). There are small (≪1 μm) zirconia inclusions throughout the material, presumably derived from the milling media that appear very bright in the backscattered electron image due to the high atomic number

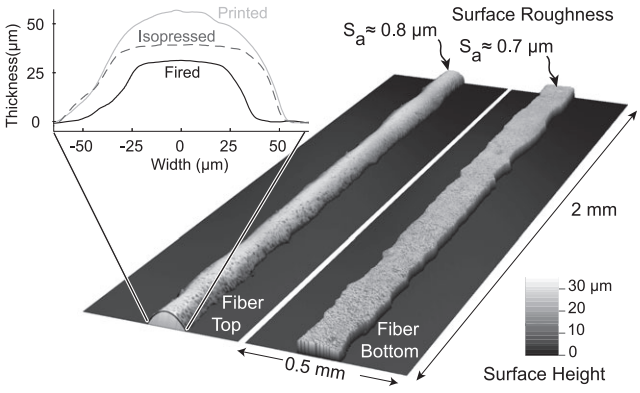


**Fig. 2.** Surface map and virtual cross sections of a fired, printed beam, gathered using interferometry.

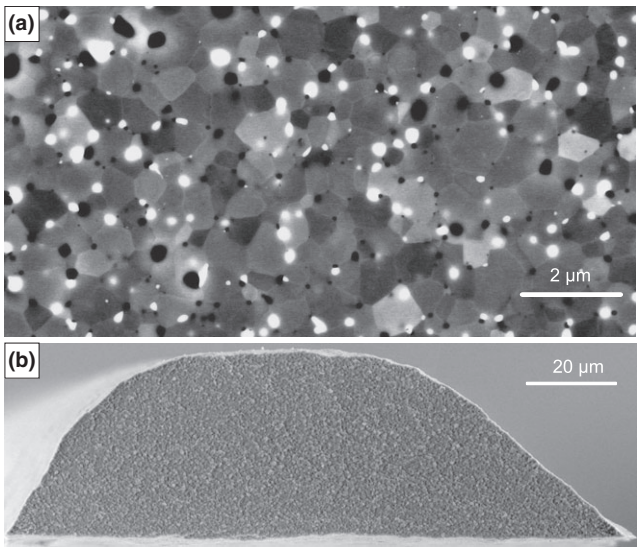


**Fig. 3.** Microstructure of printed beams. (a) Equiaxed alumina grains with 3% residual porosity (in black) and zirconia inclusions (in white). Backscattered electron image. (b) Primary fracture surface of a printed microbeam. Secondary electron image.

contrast with the alumina. Primary fracture surfaces from bend tests confirm uniform grain size and a lack of large flaws [Fig. 3(b)].

The natural frequency of mounted beams ($f_n$) was determined by inspection in the frequency domain of the step response. Neglecting damping, the system can be treated as a simple cantilever beam in mode I vibration, whence the natural frequency is as follows:

$$f_n = \frac{1.875^2}{2\pi}\sqrt{\frac{E}{\rho L^4}\frac{I}{A}}$$

where $E$ is the Young's modulus, ρ is the material density, $I$ is the moment of inertia, $A$ is the cross-section area and $L$ is the length of the cantilever. The ratio $I/A$ and $L$ were calculated numerically using virtual sections taken from the three-dimensional profilometry data. This procedure yielded specific modulus ($\bar{E} \equiv E/\rho$) values of $\bar{E} = 107 \pm 29$ GPa·m$^3$/kg, which is consistent with (though slightly higher than) that of fully dense alumina, $\bar{E}_{Al_2O_3} = 100$ GPa·m$^3$/kg.[15]

A more direct determination of the printed material modulus can be made using the Coble–Kingery relation for the modulus of porous ceramics, $E = (1 - \phi)^2 E_0$.[16] Taking the measured porosity with the intrinsic modulus of alumina ($E_0 = 400$ GPa[15]) we can estimate the modulus of the printed alumina: $E = 375$ GPa.

Flexural strengths were calculated using classic bending formulae, $\sigma_f = (My/I_x)$, with the distance from the centroid ($y$) and moment of inertia ($I_x$) computed from fractographs. The average flexural strength for *50 print pass* beams printed from 17 vol% alumina ink (our baseline configuration, with thickness of ≈25 μm) is 920 ± 190 MPa (Fig. 4).[#] The effect of solids loading in the ink is not yet understood [Fig. 4(b)], but the slight reduction of beam strength belies a degradation of printability. Although the 17 vol% ink printed repeatably at every print pass for more than 100 passes, neither of the other two formulations (13 and 23 vol%) printed reliably beyond approximately five passes.

Although the current sample size is too small for a Weibull analysis, the measured strengths can be readily compared with strength predictions for equivalent volumes

[#]Note that the tensile strength of ceramics is generally lower than the flexural strength, due to the interrogated volume and statistical population of flaws.

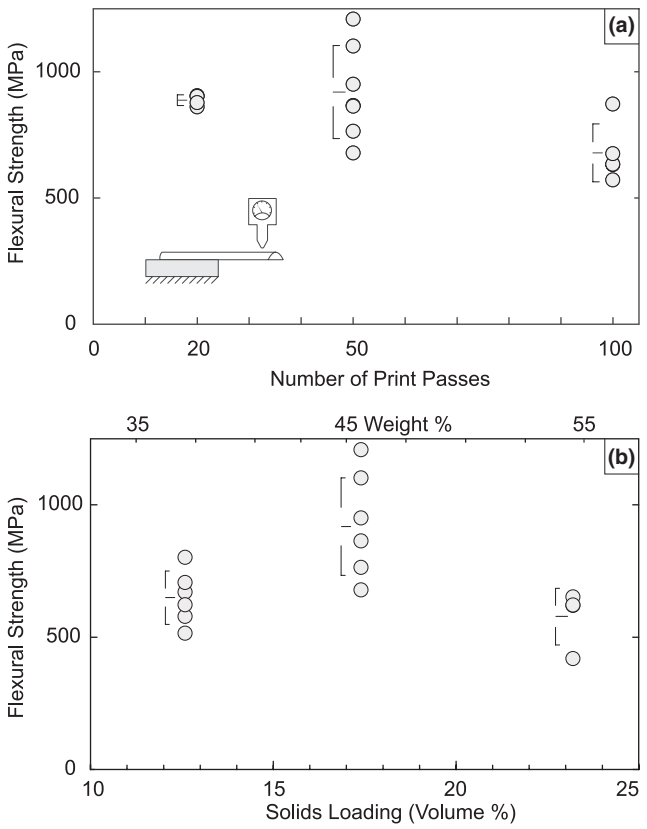


**Fig. 4.** Strength of printed alumina microbeams. (a) beams were printed with 17% alumina ink. (b) beams were printed with 50 print passes. Bars indicate average and standard deviation.

of conventionally processed alumina for which Weibull parameters have been determined. Assuming a similar specimen geometry and loading, the size-dependent strength can be calculated as[17] $\sigma_b = \sigma_a[V_a/V_b]^{1/m}$, where $\sigma$ is the flexural strength, $m$ the Weibull modulus, and $V$ the sample volume. Using typical values for conventional alumina ($m$ = 11, $\sigma_a$ = 395 MPa), and the appropriate sample volumes ($V_a$ = 3 mm × 4 mm × 20 mm = 240 mm$^3$,[17] and $V_b \approx 0.125$ mm × 0.04 mm × 20 mm = 0.1 mm$^3$ [this work]), then the threshold strength for a sample of this volume is calculated to be $\sigma_b$ = 800 MPa. This demonstrates that the ink-jet deposition process yields ceramic bodies with strength not less than conventional processing routes, but with control over shape *at very small volumes*, making such printed materials promising candidates for advanced composites.

The beam surfaces are smooth and there are no apparent deposition-related defects, such as: droplet impact artifacts (a suggested mechanism of void formation[18]), inter-splat defects, or a lamellar crack network due to poor adhesion of subsequent print passes (Figs. 2 and 3). The nature and source of the strength controlling flaws in this material are unknown, although strength and fractography indicate that critical flaw size is significantly smaller (≈5 μm for the 17 vol% ink) than the drop size (≈50 μm); a dedicated mechanistic and statistical study of this flaw population (including a Weibull analysis) will be integral to a deeper understanding of strength in printed ceramics.

Beam strength shows mild dependence on both the number of print passes and ink composition. Since the volume of interrogated material increases with beam thickness, correlation to print passes is expected. The effect of ink composition on beam strength is likely linked to printability; as the solids loading deviates from 17 vol% both the strength and printability fall off. That is, the ink no longer prints smoothly and continuously in a repeatable fashion. This indicates not only that the rheological parameters are inappropriate for printing from this cartridge, but also (and more importantly) that the ink flow is intermittent. This discontinuous flow may be due to bubble ingestions, nozzle dewetting, or a host of other inkjet phenomena, any one of which may increase defect size.

It should be noted that no effort was made to optimize the ink rheology (viscosity, surface tension, solids loading, etc.), nozzle parameters, or jetting waveform; yet high strength/high fidelity beams could be printed consistently and reliably. With some attention to ink rheology, we expect similar printability and material quality for a wide range of ink compositions.

## IV. Conclusions

Despite a crude printer and minimal ink development, a high quality ceramic material has been fabricated via inkjet printing. Although the consequences of the multilayer deposition technique are not yet fully understood, it is clear that micrometer thick layers can be assembled with minimal introduction of flaws. The inkjet printing process has demonstrated a remarkable tolerance of non-optimal fluid compositions, suggesting great potential for optimization and variety in inks. The integration of high quality ceramic into hierarchically ordered composites is under way and shows great promise for the development of tunable materials with exceptional properties.

## References

[1]E. Sachs, M. Cima, P. Williams, D. Brancazio, and J. Cornie, "Three-Dimensional Printing: Rapid Tooling and Prototypes Directly from a CAD Model," *J. Eng. Ind.*, **114** [4] 481–8 (1992).
[2]M. F. Ashby, "Hybrids to Fill Holes in Material Property Space," *Philos. Mag.*, **85** [26–27] 3235–57 (2005).
[3]J. A. Lewis, J. E. Smay, J. Stuecker, and J. Cesarano, "Direct Ink Writing of Three-Dimensional Ceramic Structures," *J. Am. Ceram. Soc.*, **89** [12] 3599–609 (2006).
[4]P. F. Blazdell, J. R. G. Evans, M. J. M. Edirisinghe, P. Shaw, and M. J. Binstead, "The Computer Aided Manufacture of Ceramics Using Multilayer Jet Printing," *J. Mater. Sci. Lett.*, **14** [22] 1562–5 (1995).
[5]B. Derby, "Inkjet Printing of Functional and Structural Materials: Fluid Property Requirements, Feature Stability, and Resolution," *Annu. Rev. Mater. Res.*, **40** [1] 395–414 (2010).
[6]B. Derby, "Inkjet Printing Ceramics: From Drops to Solid," *J. Eur. Ceram. Soc.*, **31**, 2543–50 (2011).
[7]E. Özkol, A. M. Wätjen, R. Bermejo, M. Deluca, J. Ebert, R. Danzer, and R. Telle, "Mechanical Characterisation of Miniaturised Direct Inkjet Printed 3Y-TZP Specimens for Microelectronic Applications," *J. Eur. Ceram. Soc.*, **30** [15] 3145–52 (2010).
[8]R. D. Deegan, O. Bakajin, T. F. Dupont, S. R. Nagel, and T. A. Witten, "Capillary Flow as the Cause of Ring Stains from Dried Liquid Drops," *Nature*, **389** [23] 827–9 (1997).
[9]R. Dou, T. Wang, Y. Guo, and B. Derby, "Ink-Jet Printing of Zirconia: Coffee Staining and Line Stability," *J. Am. Ceram. Soc.*, **94** [11] 3787–92 (2011).
[10]D. Soltman and V. Subramanian, "Inkjet-Printed Line Morphologies and Temperature Control of the Coffee Ring Effect," *Langmuir*, **24** [5] 2224–31 (2008).
[11]P. J. Smith, D.-Y. Shin, J. E. Stringer, B. Derby, and N. Reis, "Direct Ink-Jet Printing and Low Temperature Conversion of Conductive Silver Patterns," *J. Mater. Sci.*, **41** [13] 4153–8 (2006).
[12]E. Özkol, J. Ebert, K. Uibel, A. Watjen, and R. Telle, "Development of High Solid Content Aqueous 3Y-TZP Suspensions for Direct Inkjet Printing Using a Thermal Inkjet Printer," *J. Eur. Ceram. Soc.*, **29** [3] 403–9 (2009).
[13]J. Ebert, E. Özkol, A. Zeichner, K. Uibel, O. Weiss, U. Koops, R. Telle, and H. Fischer, "Direct Inkjet Printing of Dental Prostheses Made of Zirconia," *J. Dent. Res.*, **88** [7] 673–6 (2009).
[14]D. Wilson and L. Visser, "High Performance Oxide Fibers for Metal and Ceramic Composites," *Composites A*, **32** [8] 1143–53 (2001).
[15]W. Pabst, G. Tichá, and E. Gregorová, "Effective Elastic Properties of Alumina-Zirconia Composite Ceramics - Part 3. Calculation of Elastic Moduli of Polycrystalline Alumina and Zirconia from Monocrystal Data," *Ceram. Silik.*, **48** [2] 41–8 (2004).
[16]W. Pabst, E. Gregorova, and G. Ticha, "Elasticity of Porous Ceramics – A Critical Study of Modulus-Porosity Relations," *J. Eur. Ceram. Soc.*, **26** [7] 1085–97 (2006).
[17]R. G. Munro, "Evaluated Material Properties for a Sintered Alpha-Alumina," *J. Am. Ceram. Soc.*, **80** [8] 1919–28 (1997).
[18]J. Song and H. Nur, "Defects and Prevention in Ceramic Components Fabricated by Inkjet Printing," *J. Mater. Process. Technol.*, **155–156**, 1286–92 (2004). □